

Towards nonlinear optics with Mössbauer nuclei using x-ray cavities

Dominik Lentrodt,^{1,2,3,*} Christoph H. Keitel,³ and Jörg Evers^{3,†}

¹*Physikalisches Institut, Albert-Ludwigs-Universität Freiburg,
Hermann-Herder-Straße 3, D-79104 Freiburg, Germany*

²*EUCOR Centre for Quantum Science and Quantum Computing,
Albert-Ludwigs-Universität Freiburg, Hermann-Herder-Straße 3, D-79104 Freiburg, Germany*

³*Max-Planck-Institut für Kernphysik, Saupfercheckweg 1, 69117 Heidelberg, Germany*

Strong excitation of nuclear resonances, particularly of Mössbauer nuclei, has been a longstanding goal and the advance of novel x-ray sources is promising new options in this regard. Here we map out the necessary experimental conditions for the more general goal of realizing nonlinear optics with nuclei and compare with available technology. In particular, we present a comprehensive theory of nonlinear nuclear excitation in thin-film x-ray cavities by focused x-ray pulses. We thereby identify cavity geometries with broad resonances which allow one to boost the nuclear excitation even at moderately tight focusing and offer the possibility to mitigate radiation damage.

In this paper, we revisit an old challenge: Is it possible to fully excite an ensemble of atomic nuclei using externally applied electromagnetic fields? This question relates to the goal of building a γ -ray laser (“graser”), with inverted nuclei as a gain medium, which was proposed long ago after the laser-maser principle [1]. The discovery of the Mössbauer effect, which allows for the recoil-less absorption and emission of γ -ray photons from certain nuclei [2, 3], further fueled this research. Despite interim hope to circumvent difficulties by utilizing lasing without inversion [4], most approaches to grasing were deemed unfeasible by the late 1990s [5]. Nevertheless, recent technological and conceptual developments prompt us to reconsider the challenge.

First, advances in x-ray source technology such as x-ray free-electron lasers (XFEL) [6, 7] have promoted the study of high-energy nonlinear effects in atoms, analogous to the revolutionary development at lower photon energies following the invention of conventional laser sources [8, 9]. Various nonlinear x-ray processes have already been observed involving electronic transitions [10–14]. Closely related to the original question, also lasing on an inner-shell electronic transition based on XFEL-generated inversion has been demonstrated [15]. This raises the question if the source advances provide new avenues for the excitation of nuclei.

Second, Mössbauer nuclei by now have evolved into a promising platform for quantum optics at energies of hard x-rays. In a series of experiments, key concepts of quantum optics [16–22] and coherent control [23–30] have been demonstrated with nuclei as the matter part. However, while these experiments exploit coherence and interference effects and demonstrate a surprising level of control, they still operate in the linear optics regime, such that they can be described by (semi-)classical optics calculations [31, 32].

These two developments also motivate a shift in focus away from the goal of reaching full inversion and towards more general nonlinear optics effects, further fueled by recent experiments from the optical domain [33–37] demon-

strating that effects such as photon correlations can already appear far below full excitation. First experiments with Mössbauer nuclei at XFELs [38, 39] explore this direction, e.g. by scattering multiple photons per shot [38]. Still these experiments do not reach beyond linear optics, which remains an open challenge.

On the theoretical side, a number of schemes have been proposed to achieve higher excitation or get close to the inversion threshold. For example, it has been suggested to overcome discouraging first estimates [40] using additional accelerations of the target nuclei [41], non-dipole transitions [42], or collective effects in the light-matter interaction [43, 44]. Furthermore, there are multiple approaches to boost the excitation of the nuclei by a suitable tailoring of their electromagnetic environment. As one option, front-coupling in one-dimensional x-ray waveguides is well-studied for imaging applications [45, 46], has recently been implemented with nuclei [47, 48], and tapered variants have been suggested as a candidate for nuclear inversion [49, 50]. Alternatively, x-ray thin-film planar cavities containing layers of Mössbauer nuclei are well established as a major platform for nuclear quantum optics in the linear regime [51, 52]. The field enhancement inside such structures has been considered [16, 31, 53–55] and optimized [46, 56]. However, the latter works consider the state-of-the-art probing using highly collimated x-rays, which is unfavorable for strong excitation. Focusing to enhance the nuclear excitation has been proposed [57], but so far, rigorous modelling of the excitation dynamics in planar waveguides driven by focused x-ray beams and a corresponding roadmap towards nonlinear excitation are missing.

In this Letter, we utilize a comprehensive theory developed in a companion paper [58] to study the excitation dynamics of Mössbauer nuclei in planar cavities driven by focused x-ray pulses (see Fig. 1). We find that the rigorous modeling of the focusing leads to optimum cavity structures which qualitatively differ from well-established design paradigms for collimated x-ray beams. The latter may even lead to an excitation performance worse

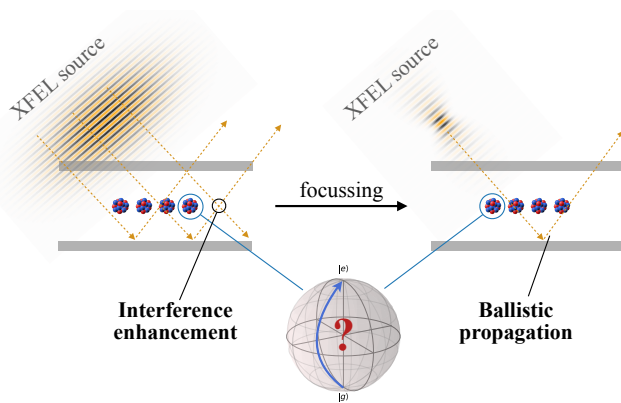


FIG. 1. Sketch of the setup, featuring a focused x-ray pulse (not to scale) incident on a thin-film cavity doped with narrow resonances, such as Mössbauer nuclei. By focusing the incident x-ray pulse, one can concentrate the radiation on fewer nuclei, potentially increasing their excitation towards inversion (illustrated by the Bloch sphere). However, this comes at the cost of reducing the cavity enhancement from interference. We show that using suitably designed cavities, this limitation can be overcome in intermediate focusing regimes and map out which configurations are most advantageous for upcoming experiments.

than without the cavity. With varying size of the x-ray focus, we identify a transition between standing-wave interference and ballistic reflections, with significant field enhancement down to moderately tight focusing. We calculate the necessary source parameters to enter the nonlinear regime of significantly excited nuclei and demonstrate its feasibility by comparing with currently available conditions and planned upgrades.

We start with the nuclear excitation dynamics. Unlike in the low-excitation regime [55, 59], the modeling of dissipative quantum dynamics of many interacting few-level systems at higher excitation remains a challenging problem of much current interest [60–62]. However, x-ray pulses delivered by accelerator-based sources are orders of magnitude shorter (typically ps to fs scale) than any other relevant time scale in the nuclear dynamics (e.g., ns for ^{57}Fe). This allows one to separate the excitation from the subsequent decay dynamics. The former then essentially reduces to a single-particle problem (see [58] for details), since dissipative and coupling processes are ineffective over the short excitation time scales.

The single-nucleus dynamics can straightforwardly be solved numerically for arbitrary input fields. However, to gain analytical insight, we further assume resonant and Fourier-limited x-ray pulses, an idealization of pulses generated via hard x-ray self-seeding [63–65]. Then, the pulse area theorem [66–68] relates the nuclear state after the x-ray pulse to the Fourier transform of the x-ray field at the nuclear resonance frequency $\mathbf{E}_{\text{drive}}(\mathbf{r}_{\text{nuc}}, \omega_{\text{nuc}})$

as [58, 69]

$$\Phi = \frac{4\pi}{\hbar} |\mathbf{d} \cdot \mathbf{E}_{\text{drive}}(\mathbf{r}_{\text{nuc}}, \omega_{\text{nuc}})|. \quad (1)$$

Here, Φ is the so-called pulse area, and \mathbf{d} , \mathbf{r}_{nuc} , and ω_{nuc} are the electric dipole moment (an effective quantity for magnetic transitions), the position and the transition frequency of the nuclei, respectively. The nuclear excitation — which is directly related to the magnitude of many nonlinear processes — is then obtained as $\sigma^z = -\cos(\Phi)$, where σ^z is the expectation value of the transition’s Pauli operator.

An intuitive interpretation is gained by rewriting Eq. (1) [58] as

$$\Phi = \frac{\chi_\sigma}{w_0} \cdot \chi_{\text{source}} \cdot \xi_\mathcal{E}, \quad (2)$$

where χ_σ is a transition characteristic that solely depends on the nuclear properties such as the dipole moment. w_0 is the beam waist size in the focal plane, characterizing the strength of the focusing. The incident x-ray pulses are characterized by their pulse energy E_{pulse} and relative bandwidth b_r via $\chi_{\text{source}} := \sqrt{E_{\text{pulse}}/b_r}$. Finally, $\xi_\mathcal{E}$ is an enhancement factor due to the cavity. Without cavity — that is in free space — it is equal to unity. Therefore, the goal of the cavity environment is to increase $\xi_\mathcal{E}$. From the criterion $\Phi = \pi$ for reaching inversion, we define a *necessary* source characteristic for a given nucleus, cavity and focusing as

$$\chi_{\text{source}}^{\text{nec}} = \pi \frac{w_0}{\chi_\sigma \xi_\mathcal{E}}. \quad (3)$$

For a given χ_{source} , one can then express the achievable nuclear excitation as $\sigma^z = -\cos\left(\frac{\pi \chi_{\text{source}}}{\chi_{\text{source}}^{\text{nec}}}\right)$.

The crucial position-dependent enhancement factor $\xi_\mathcal{E}(\mathbf{r})$ is obtained by calculating the propagation of focused x-ray pulses in the cavity medium using Maxwell’s equations. In the companion paper [58], an efficient semi-analytical algorithm specialized for this purpose is developed, which forms the basis of the results below.

We start with the discussion of a standard cavity design [16, 70]. Results are shown in Fig. 2. Panel (a) depicts the electronic reflectance as a function of grazing incidence angle (rocking curve), featuring two cavity resonances. Following standard design criteria, the first resonance is relatively narrow and critically coupled [16, 46, 56]. The latter condition implies a vanishing of the resonant electronic reflectance, such that the isolated response of the nuclei inside the cavity can experimentally be accessed [71].

Panel (b) shows the spatially-resolved cavity enhancement factor inside and outside the cavity for three different x-ray input fields (top to bottom). Their incidence angles are all on resonance with the first cavity mode, but they feature different focusing strengths. The corresponding beam divergences $\theta_{\text{div}} = 0.3, 0.685$ and 2.0 mrad are

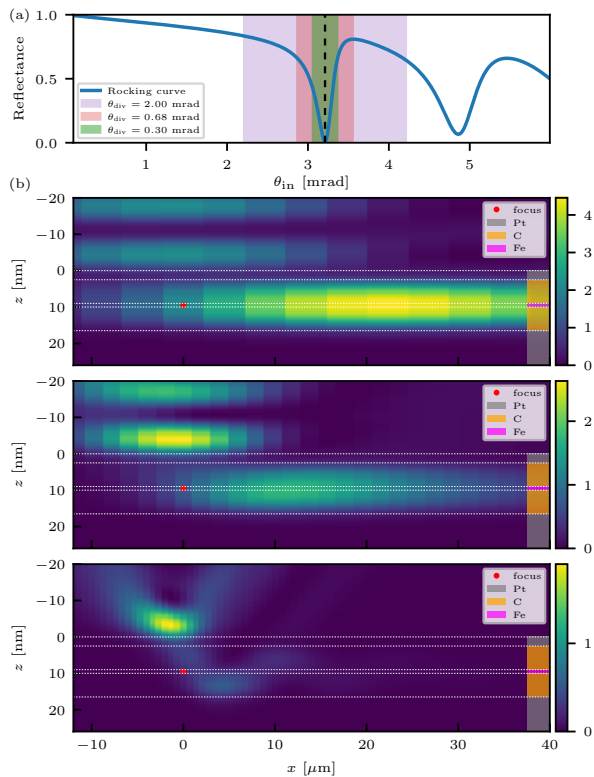


FIG. 2. Results for an example cavity following standard design criteria. (a) Electronic reflection as a function of incidence angle (rocking curve). The shaded areas indicate three different input beam divergence ranges considered in panel (b), see legend. (b) Spatially resolved cavity enhancement factor $\xi_{\mathcal{E}}$ in and around the example cavity (cladding boundary at $z = 0$) for the beam divergences $\theta_{\text{div}} = 0.3, 0.685$ and 2.0 mrad (top to bottom), where the middle value corresponds to 40 nm spot size. The incident beam propagates from the top left to the bottom right and encounters the cavity starting from $z = 0$. The colored areas and white horizontal lines indicate the location of the cavity layers (see legend). The red dot indicates the free-space beam focus, which is placed at the depth of the nuclear ensemble. Intensities are normalized to corresponding free-space intensity maxima.

indicated as shaded regions in (a). x is the projection of the pulse propagation direction onto the waveguide surface, and z the surface normal.

At low focusing (panel b, top), the field enhancement inside the cavity is clearly visible, arising from the constructive interference of multiple x-ray reflections. As desired, the intensity maximum is at the position of the nuclei. Above the cavity surface, a standing wave pattern appears from the interference of in- and outgoing x-ray fields.

Towards higher focusing [panel (b), top to bottom] the intensity enhancement reduces. On the one hand, with increasing beam divergence, a growing part of the incident wave vector components is off-resonant and cannot contribute to the standing wave enhancement. Also,

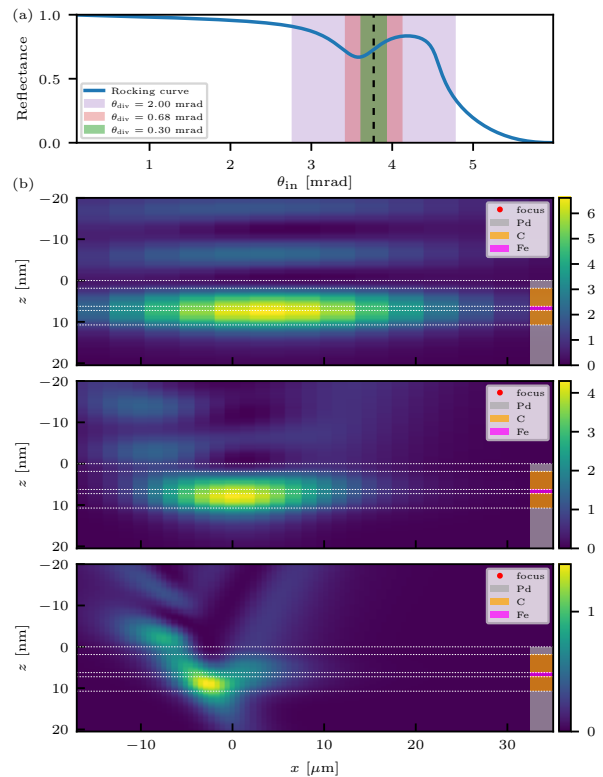


FIG. 3. Analogous to Fig. 2, but for a cavity optimized for a focal spot size of 40 nm. The resonance structure in this case is rather different from the standard cavity, with a broad resonance far from critical coupling. However, such a cavity allows to obtain field enhancement at the resonant ensemble location (magenta) even for tight focusing. Note that the free-space focus is located above the plot limits at 33.2 nm as a result of the optimization.

however, the focused wave packets become smaller such that the spatial overlap of the different reflections diminishes, again impeding the constructive interference leading to the intensity enhancement. The latter effect is visible in the highly focused case (b, bottom), and implies a practical lower spot-size limit for the focusing. In addition to the enhancement reduction, most of the wave packet is reflected already at the outer cladding, such that the maximum field intensity is shifted to the outside of the cavity structure. Thus, the intensity at the nuclei's positions is in fact lower than it would be in the absence of the cavity.

From these results, we conclude that standard cavity designs are unsuitable in combination with focusing. However, these limitations can be overcome using alternative cavity designs. To this end, we choose a moderately strong focusing spot size of 40 nm and optimized the cavity layer structure for maximum intensity enhancement at the position of the nuclei [70]. The results in this case are shown in Fig. 3. In comparison to the standard cavity in Fig. 2, we observe two qualitative differences.

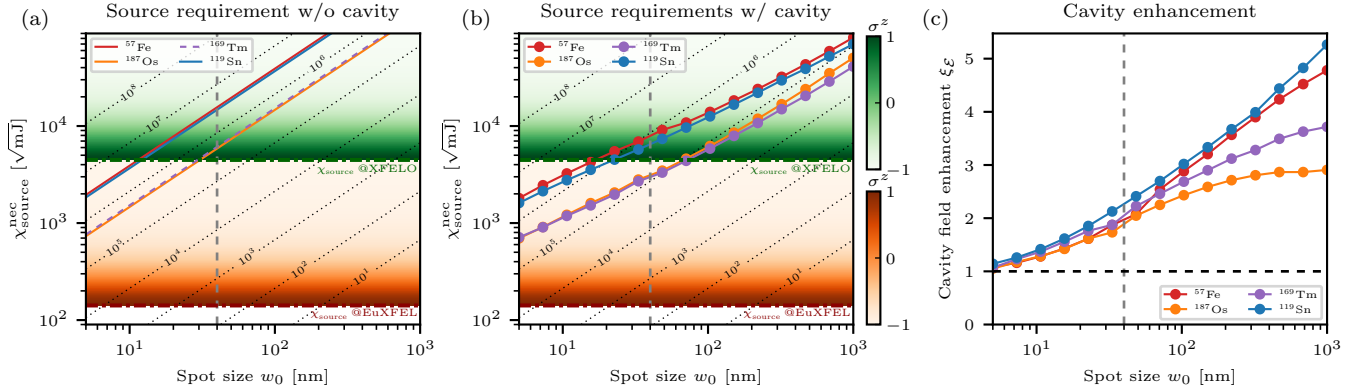


FIG. 4. Source requirements necessary for inversion as a function of the beam spot size, expressed as the necessary source characteristic $\chi_{\text{source}}^{\text{necc}} = \sqrt{E_{\text{pulse}}^{\text{necc}}/b_r^{\text{necc}}}$. Panel (a) shows results for each isotope (lines; see legend) in free space. Panel (b) shows corresponding results with a cavity environment optimized for enhancement at each spot size (optimization points marked by dots; lines provided as a guide for the eye). The vertical dashed line indicates a potentially achievable spot size of 40 nm. Panel (c) shows the corresponding cavity enhancement factor. For comparison to practical conditions, the available χ_{source} at the European XFEL (horizontal red dash-dotted line) and at the planned oscillator upgrade [70] (horizontal green dash-dotted line) are shown in (a) and (b). Inversion is then realized when χ_{source} and $\chi_{\text{source}}^{\text{necc}}$ cross. As additional information, the background shading (red and green, respectively) indicates the achievable excitation if χ_{source} lies below $\chi_{\text{source}}^{\text{necc}}$, that is for sub-inversion conditions. The color axis then corresponds to $\sigma^z = -\cos\left(\frac{\pi\chi_{\text{source}}}{\chi_{\text{source}}^{\text{necc}}}\right)$ [colorbars in panel (b)] at a given necessary [$\chi_{\text{source}}^{\text{necc}}$] and actual [χ_{source}] source parameter for the respective sources [70]. The physically relevant value is then the shading at the point of the corresponding $\chi_{\text{source}}^{\text{necc}}$ -line and indicates the expected strength of nonlinear effects which are achievable with each Mössbauer isotope (see legend) at this source. Similarly, the diagonal dotted lines indicate contours of x-ray fluences per pulse bandwidth at the cavity surface [units of $\frac{\mu\text{J}}{\mu\text{m}^2\text{meV}}$], which allow to estimate the radiation damage on the targets.

First, the rocking curve in panel (a) features a relevant resonance which is rather weak and surprisingly broad. Second, the optimized cavity [structure see Fig. 3, panel (a)] enables a significant intensity enhancement even at higher focusing [panel (b), top to bottom], and the x-rays are mostly reflected from the substrate rather than from the surface, which boosts the excitation at the nuclear position. This improvement is due to the larger acceptance angle of broader cavity resonances.

After discussing the qualitative aspects of focusing on the nuclear excitation dynamics, we now turn to quantitative predictions for the Mössbauer isotopes ^{57}Fe , ^{187}Os , ^{169}Tm and ^{119}Sn . To this end, we determine the necessary source parameter $\chi_{\text{source}}^{\text{necc}}$ to reach nuclear inversion as a function of the free-space beam spot size w_0 for each of these isotopes. For comparison, we further indicate the source conditions available at the European XFEL [72–75] and the projected conditions at the planned oscillator upgrade [76] (detailed data tables are provided in [58]).

Results are shown in Fig. 4. As a reference, panel (a) illustrates the case without cavity environment, for which $\chi_{\text{source}}^{\text{necc}} \propto \omega_{\text{nuc}}$. In the relevant hard x-ray energy range, nano-focusing setups at EuXFEL beamlines currently offer spot sizes down to about 40 nm [77], which is indicated as a vertical dashed line. At this focusing strength, present-day beam conditions at EuXFEL are still far below the requirements for full inversion. How-

ever, XFELo conditions [76] already approach the required χ_{source} values and significant σ^z can be reached, indicating the onset of the nonlinear regime.

Panel (b) shows corresponding results with waveguide enhancements. To this end, we optimized the cavity structure for maximum excitation enhancement at each spot size using the algorithm developed in the companion paper [58]. We see that the cavity enhancement indeed allows one to reduce the source requirements, such that the projected XFELo parameters even exceed the requirements for inversion in ^{187}Os and ^{169}Tm . The relative improvement by the cavity is quantified in panel (c), which shows the ratios of the required source parameters with and without cavity as a function of focusing spot size, which is equal to the cavity field enhancement $\xi_{\mathcal{E}}$. We see that enhancements in the pulse area are possible even at substantial focusing. Note that away from full inversion, which presently is experimentally most relevant, the excitation scales quadratically with the pulse area, such that nonlinear effects are also enhanced quadratically.

In addition to the available source and focusing conditions, an important practical question is whether the target can survive possible radiation damage. To this end, Fig. 4 also shows the fluences per pulse bandwidth on the sample surface. Damage thresholds of materials in the x-ray regime have been much investigated (see

e.g. [78, 79]) and typical values in combination with Fig. 4 indicate that experiments may be feasible depending on the level of monochromatization. Alternatively, the small focal spot can be scanned across the cavity surface from x-ray pulse to pulse. In any case, the focusing strength plays a crucial role with regards to practical feasibility: a stronger focus is necessary for strong excitation, but simultaneously increases radiation damage. However, Fig. 4 shows that cavities can further help in this regard, since in free space, the fluence contours have the same slope as the excitation contours, but for the optimized cavities, the slope of the latter is changed.

In summary, we have shown that optimized thin-film cavities provide means to significantly boost Mössbauer nuclei towards the nonlinear optics regime, in particular for conditions much below inversion and even for tight focusing. The enhancement can be interpreted as a longitudinal compression of the pulse via the multi-path interference in the cavity. In this sense, cavities are complementary to focusing techniques, which provide a transversal compression of the light field. We find that by combining both effects, the optimum cavity designs qualitatively differ from state-of-the-art designs for collimated x-ray beams and optimized the cavity geometry to achieve significant enhancements down to 40 nm focusing. With planned upgrades to currently available sources, the resulting enhancement enables excitation of nuclei into the nonlinear regime. In particular for the isotopes ^{187}Os and ^{169}Tm , inversion is predicted to be achievable and ^{57}Fe — the workhorse of Mössbauer science — is boosted to significantly nonlinear excitation fractions. Our results thereby outline a roadmap for further source developments and experimental efforts, balancing between advances in pulse energy and focusing capabilities. Progressing beyond the state-of-the-art linear regime would then allow to explore the linear quantum optical effects already observed with nuclei [16–22, 24, 28] in an as-yet unexplored parameter regime and potentially enable the creation of correlated x-ray photons [35–37].

The authors would like to thank K. P. Heeg, O. Diekmann, M. Gerharz, R. Röhlberger and L. Wolff for valuable discussions and L. M. Lohse for comments on an earlier version of the manuscript. DL gratefully acknowledges the Georg H. Endress Foundation for financial support and support by the DFG funded Research Training Group “Dynamics of Controlled Atomic and Molecular Systems” (RTG 2717).

We note that this paper is based on the doctoral thesis [80]. The software and figures in this paper made use of the NUMPY [81], SCIPY [82] and MATPLOTLIB [83] software packages.

End Matter

To supplement the discussion in the main text, Fig. 5 shows analogous results to Fig. 4 for a fixed cavity. That is instead of optimizing the cavity structure for each spot size, the behavior of the cavity optimized for a spot size of 40 nm is investigated. In this case, the cavity enhancement levels off more rapidly, such that the necessary source parameter scales the same way as the radiation damage starting at a spot size of around 70 nm. This observation further illustrates how optimized cavities can be useful to mitigate radiation damage.

Details on the cavity optimization

In the optimization procedure, we use the algorithm developed in [?], which allows to compute the effect of the cavity on the pulse area of a focused x-ray pulse. The input pulse is a Gaussian beam [?] with a given beam divergence θ_{div} and incidence angle θ_{in} .

For the optimization, we fix the beam divergence such that the spot size of the beam is 40 nm. The cavity geometry to be optimized is assumed to have the form $m_{\text{clad}}(d_1)/C(d_2)/m_{\text{res}}(1\text{ nm})/C(d_3)/m_{\text{clad}}(\infty)$. For the cladding materials, we allowed for $m_{\text{clad}} \in \{\text{Pt}, \text{Pd}\}$. d_1, d_2, d_3 were optimized as free parameters together with the incidence angle θ_{in} and the focusing height z_{focus} . That is, the geometry to be optimized is restricted to a cladding/guiding layer/substrate structure with a 1 nm resonant layer inside the guiding layer. More complicated multi-layer structures are not allowed for and subject to future investigation.

The optimization was then performed in PYTHON [?] using the dual annealing global optimizer from the SCIPY.OPTIMIZE [82] package. Note that previous work on optimized x-ray cavity resonances includes the general study [46]. Our algorithm is designed for the particular purpose of nonlinear nuclear excitation and includes various analytical approximations that increase the efficiency.

Data tables

Tables I-III contains the data used for the inversion prediction as a reference. Each table was automatically generated using the code which was used to create Fig. 4 in the main text.

* dominik.lentrodt@physik.uni-freiburg.de

† joerg.evers@mpi-hd.mpg.de

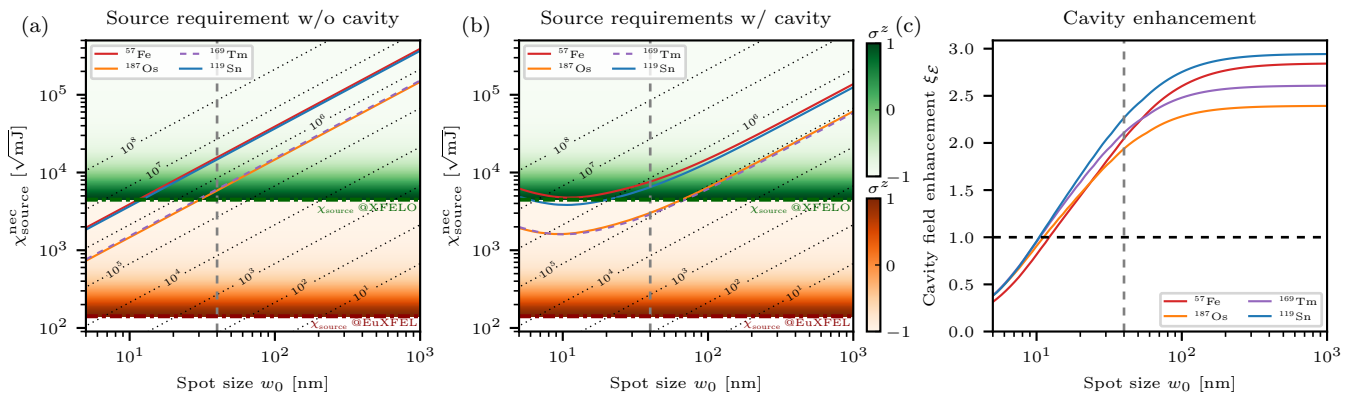


FIG. 5. Source requirements for a specified cavity. This figure is analogous to Fig. 4, but uses a single cavity geometry optimized for a spot size of 40 nm focusing instead of at each spot size in order to illustrate the behavior of the cavity structures discussed in the main text.

- [1] G. C. Baldwin, J. C. Solem, and V. I. Gol'danskii, *Approaches to the development of gamma-ray lasers*, Rev. Mod. Phys. **53**, 687 (1981).
- [2] R. L. Mössbauer, *Kernresonanzfluoreszenz von gammastrahlung in ir191*, Zeitschrift für Physik **151**, 124 (1958).
- [3] R. L. Mössbauer, *Recoilless nuclear resonance absorption of gamma radiation*, Science **137**, 731 (1962), <https://science.sciencemag.org/content/137/3532/731.full.pdf>.
- [4] O. Kocharovskaya, *Amplification and lasing without inversion*, Physics Reports **219**, 175 (1992).
- [5] G. C. Baldwin and J. C. Solem, *Recoilless gamma-ray lasers*, Rev. Mod. Phys. **69**, 1085 (1997).
- [6] C. Pellegrini, A. Marinelli, and S. Reiche, *The physics of x-ray free-electron lasers*, Rev. Mod. Phys. **88**, 015006 (2016).
- [7] I. Georgescu, *The first decade of xfels*, Nature Reviews Physics **2**, 345 (2020).
- [8] A. L. Schawlow and C. H. Townes, *Infrared and optical masers*, Phys. Rev. **112**, 1940 (1958).
- [9] W. E. Lamb, W. P. Schleich, M. O. Scully, and C. H. Townes, *Laser physics: Quantum controversy in action*, Rev. Mod. Phys. **71**, S263 (1999).
- [10] I. Matsuda and R. Arafune, eds., *Nonlinear X-ray spectroscopy for materials science*, Springer series in optical sciences, Vol. 246 (Springer, Singapore, 2023) pp. xiv, 160 pages : illustrations, diagrams.
- [11] N. Rohringer, *X-ray raman scattering: a building block for nonlinear spectroscopy*, Philosophical Transactions of the Royal Society A: Mathematical, Physical and Engineering Sciences **377**, 20170471 (2019).
- [12] S. Sofer, E. Strizhevsky, A. Schori, K. Tamasaku, and S. Schwartz, *Quantum enhanced x-ray detection*, Phys. Rev. X **9**, 031033 (2019).
- [13] S. Nandi, E. Olofsson, M. Bertolino, S. Carlström, F. Zapata, D. Busto, C. Callegari, M. Di Fraia, P. Eng-Johnsson, R. Feifel, G. Gallician, M. Gisselbrecht, S. Maclot, L. Neoričić, J. Peschel, O. Plekan, K. C. Prince, R. J. Squibb, S. Zhong, P. V. Demekhin, M. Meyer, C. Miron, L. Badano, M. B. Danailov, L. Giannessi, M. Manfreda, F. Sottocorona, M. Zangrando, and J. M. Dahlström, *Observation of rabi dynamics with a short-wavelength free-electron laser*, Nature **608**, 488 (2022).
- [14] G. Doumy, C. Roedig, S.-K. Son, C. I. Blaga, A. D. DiChiara, R. Santra, N. Berrah, C. Bostedt, J. D. Bozek, P. H. Bucksbaum, J. P. Cryan, L. Fang, S. Ghimire, J. M. Glowia, M. Hoener, E. P. Kanter, B. Krässig, M. Kuebel, M. Messerschmidt, G. G. Paulus, D. A. Reis, N. Rohringer, L. Young, P. Agostini, and L. F. DiMauro, *Nonlinear atomic response to intense ultrashort x rays*, Phys. Rev. Lett. **106**, 083002 (2011).
- [15] N. Rohringer, D. Ryan, R. A. London, M. Purvis, F. Albert, J. Dunn, J. D. Bozek, C. Bostedt, A. Graf, R. Hill, S. P. Hau-Riege, and J. J. Rocca, *Atomic inner-shell x-ray laser at 1.46 nanometres pumped by an x-ray free-electron laser*, Nature **481**, 488 (2012).
- [16] R. Röhlberger, K. Schlage, B. Sahoo, S. Couet, and R. Rüffer, *Collective lamb shift in single-photon superradiance*, Science **328**, 1248 (2010).
- [17] R. Röhlberger, H.-C. Wille, K. Schlage, and B. Sahoo, *Electromagnetically induced transparency with resonant nuclei in a cavity*, Nature **482**, 199 (2012).
- [18] K. P. Heeg, H.-C. Wille, K. Schlage, T. Guryeva, D. Schumacher, I. Uschmann, K. S. Schulze, B. Marx, T. Kämpfer, G. G. Paulus, R. Röhlberger, and J. Evers, *Vacuum-assisted generation and control of atomic coherences at x-ray energies*, Phys. Rev. Lett. **111**, 073601 (2013).
- [19] K. P. Heeg, C. Ott, D. Schumacher, H.-C. Wille, R. Röhlberger, T. Pfeifer, and J. Evers, *Interferometric phase detection at x-ray energies via Fano resonance control*, Phys. Rev. Lett. **114**, 207401 (2015).
- [20] K. P. Heeg, J. Haber, D. Schumacher, L. Bocklage, H.-C. Wille, K. S. Schulze, R. Loetzsch, I. Uschmann, G. G. Paulus, R. Rüffer, R. Röhlberger, and J. Evers, *Tunable subluminal propagation of narrow-band x-ray pulses*, Phys. Rev. Lett. **114**, 203601 (2015).
- [21] J. Haber, K. S. Schulze, K. Schlage, R. Loetzsch, L. Bocklage, T. Guryeva, H. Bernhardt, H.-C. Wille, R. Rüffer, I. Uschmann, G. G. Paulus, and R. Röhlberger, *Collective strong coupling of x-rays and nuclei in a nuclear optical lattice*, Nat. Phot. **10**, 445 EP (2016).
- [22] J. Haber, X. Kong, C. Strohm, S. Willing, J. Gollwitzer, L. Bocklage, R. Rüffer, A. Pálffy, and R. Röhlberger, *Rabi oscillations of x-ray radiation between two nuclear ensembles*, Nat. Phot. **11**, 720 (2017).

	Z	A	E [keV]	γ [neV]	α	Multipolarity	I_g	I_e	d_{eff} [C·m]	$\sqrt{\sigma_{\text{nuc}}}$ [nm]	σ_{nuc} [nm ²]	σ_{nuc} [kbarn]
⁵⁷ Fe	26	57	14.41	4.66	8.6	M1	0.5	1.5	3.34E-36	6.31E-09	3.99E-17	3.99E-10
¹⁹³ Pt	78	193	1.64	47.00	3.5	M1	1.5	0.5	2.01E-34	3.81E-07	1.45E-13	1.45E-06
¹⁸⁷ Os	76	187	9.75	191.70	264.0	M1	0.5	1.5	7.31E-36	1.38E-08	1.91E-16	1.91E-09
¹⁶⁹ Tm	69	169	8.41	106.00	285.0	M1	0.5	1.5	6.53E-36	1.23E-08	1.52E-16	1.52E-09
¹¹⁹ Sn	50	119	23.87	25.70	5.2	M1	0.5	1.5	4.56E-36	8.62E-09	7.43E-17	7.43E-10

TABLE I. Isotope properties used for the inversion prediction. This table was generated automatically with the simulation code used for Fig. 4 and is printed here as a reference. Base parameters are sourced from [31, 57].

	Pt (δ)	Pt (β)	C (δ)	C (β)	res (δ)	res (β)	Pd (δ)	Pd (β)
⁵⁷ Fe	1.6E-05	2.6E-06	2.3E-06	1.2E-09	7.2E-06	3.3E-07	1.0E-05	3.4E-07
¹⁹³ Pt	8.7E-04	2.1E-04	1.7E-04	7.4E-06	1.3E-03	2.1E-04	7.0E-04	1.5E-04
¹⁸⁷ Os	3.5E-05	2.6E-06	4.9E-06	5.4E-09	4.0E-05	2.4E-06	2.3E-05	1.4E-06
¹⁶⁹ Tm	4.7E-05	4.4E-06	6.6E-06	9.9E-09	2.2E-05	1.3E-06	3.1E-05	2.5E-06
¹¹⁹ Sn	6.2E-06	4.2E-07	8.2E-07	2.8E-10	2.2E-06	3.7E-08	3.5E-06	5.2E-08

TABLE II. Refractive indices at each isotope's transition energy (see Table I) used for the inversion prediction. This table was generated automatically with the simulation code used for Fig. 4 and is printed here as a reference. Numbers are sourced from [32? ? ?].

	Layer 1	Layer 2	Layer 3	Layer 4	Layer 5	θ_{in} [mrad]	z_{foc} [nm]
⁵⁷ Fe	Pd (1.87 nm)	C (4.37 nm)	Fe (1.00 nm)	C (2.59 nm)	Pd (∞)	3.771	33.2
¹⁹³ Pt	Pd (2.50 nm)	C (3.50 nm)	Pt (1.00 nm)	C (3.50 nm)	Pd (∞)	33.110	0.0
¹⁸⁷ Os	Pt (1.55 nm)	C (3.64 nm)	Os (1.00 nm)	C (2.34 nm)	Pt (∞)	6.888	28.6
¹⁶⁹ Tm	Pt (1.49 nm)	C (3.30 nm)	Tm (1.00 nm)	C (2.44 nm)	Pt (∞)	7.494	28.3
¹¹⁹ Sn	Pt (1.78 nm)	C (2.86 nm)	Sn (1.00 nm)	C (2.20 nm)	Pt (∞)	2.727	30.0

TABLE III. Optimized cavity and focusing parameters used for the inversion prediction. This table was generated automatically with the simulation code used for Fig. 4 and is printed here as a reference.

	E_{pulse} [mJ]	b_r (EuXFEL)	b_r (EuXFELo, projected)
⁵⁷ Fe	2.00E+00	1.00E-04	1.00E-07
¹⁹³ Pt	2.00E+00	1.00E-04	1.00E-07
¹⁸⁷ Os	2.00E+00	1.00E-04	1.00E-07
¹⁶⁹ Tm	2.00E+00	1.00E-04	1.00E-07
¹¹⁹ Sn	2.00E+00	1.00E-04	1.00E-07

TABLE IV. Source parameters used for the horizontal lines in Fig. 4. The input parameters are E_{pulse} and b_r , which can be converted into the other shown parameters for a Gaussian pulse. This table was generated automatically with the simulation code used for Fig. 4 and is printed here as a reference. Numbers are sourced from [77], the oscillator upgrade values are estimates from [76].

- [23] P. Helistö, I. Tittonen, M. Lippmaa, and T. Katila, *Gamma echo*, Phys. Rev. Lett. **66**, 2037 (1991).
- [24] Y. V. Shvyd'ko, T. Hertrich, U. van Bürck, E. Gerdau, O. Leupold, J. Metge, H. D. Rüter, S. Schwendy, G. V. Smirnov, W. Potzel, and P. Schindelmann, *Storage of nuclear excitation energy through magnetic switching*, Phys. Rev. Lett. **77**, 3232 (1996).
- [25] P. Schindelmann, U. van Bürck, W. Potzel, G. V. Smirnov, S. L. Popov, E. Gerdau, Y. V. Shvyd'ko, J. Jäschke, H. D. Rüter, A. I. Chumakov, and R. Ruffer, *Radiative decoupling and coupling of nuclear oscillators by stepwise doppler-energy shifts*, Phys. Rev. A **65**, 023804 (2002).
- [26] F. Vagizov, V. Antonov, Y. V. Radeonychev, R. N. Shakhmuratov, and O. Kocharovskaya, *Coherent control of the waveforms of recoilless g-ray photons*, Nature **508**, 80 (2014).
- [27] S. Sakshath, K. Jenni, L. Scherthan, P. Würtz, M. Herlitschke, I. Sergeev, C. Strohm, H.-C. Wille, R. Röhlsberger, J. A. Wolny, and V. Schünemann, *Optical pump - nuclear resonance probe experiments on spin crossover complexes*, Hyperfine Interactions **238**, 89 (2017).
- [28] K. P. Heeg, A. Kaldun, C. Strohm, P. Reiser, C. Ott, R. Subramanian, D. Lentrodt, J. Haber, H.-C. Wille, S. Goerttler, R. Ruffer, C. H. Keitel, R. Röhlsberger, T. Pfeifer, and J. Evers, *Spectral narrowing of x-ray pulses for precision spectroscopy with nuclear resonances*, Science **357**, 375 (2017).
- [29] K. P. Heeg, A. Kaldun, C. Strohm, C. Ott, R. Subramanian, D. Lentrodt, J. Haber, H.-C. Wille, S. Goerttler, R. Ruffer, C. H. Keitel, R. Röhlsberger, T. Pfeifer, and J. Evers, *Coherent x-ray-optical control of nuclear excitons*, Nature **590**, 401 (2021).
- [30] L. Bocklage, J. Gollwitzer, C. Strohm, C. F. Adolff, K. Schlage, I. Sergeev, O. Leupold, H.-C. Wille, G. Meier, and R. Röhlsberger, *Coherent control of collective nuclear quantum states via transient magnons*, Science Advances **7** (2021), 10.1126/sciadv.abc3991, <https://advances.sciencemag.org/content/7/5/eabc3991.full.pdf>.
- [31] R. Röhlsberger, *Nuclear Condensed Matter Physics with Synchrotron Radiation*, Springer Tracts in Modern Physics, Vol. 208 (Springer, Berlin, Heidelberg, 2005).
- [32] W. Sturhahn, *Conuss and phoenix: Evaluation of nuclear resonant scattering data*, Hyperfine Interactions **125**, 149 (2000).
- [33] M. T. Manzoni, D. E. Chang, and J. S. Douglas, *Simulating quantum light propagation through atomic ensembles using matrix product states*, Nature Communications **8**, 1743 (2017).
- [34] S. Mahmoodian, M. Čepulkovskis, S. Das, P. Lodahl, K. Hammerer, and A. S. Sørensen, *Strongly correlated photon transport in waveguide quantum electrodynamics with weakly coupled emitters*, Phys. Rev. Lett. **121**, 143601 (2018).
- [35] A. S. Prasad, J. Hinney, S. Mahmoodian, K. Hammerer, S. Rind, P. Schneeweiss, A. S. Sørensen, J. Volz, and A. Rauschenbeutel, *Correlating photons using the collective nonlinear response of atoms weakly coupled to an optical mode*, Nature Photonics **14**, 719 (2020).
- [36] M. Cordier, M. Schemmer, P. Schneeweiss, J. Volz, and A. Rauschenbeutel, *Tailoring photon statistics with an atom-based two-photon interferometer*, Phys. Rev. Lett. **131**, 183601 (2023).
- [37] C. Liedl, F. Tebbenjohanns, C. Bach, S. Pucher, A. Rauschenbeutel, and P. Schneeweiss, *Observation of superradiant bursts in a cascaded quantum system*, Phys. Rev. X **14**, 011020 (2024).
- [38] A. I. Chumakov, A. Q. R. Baron, I. Sergueev, C. Strohm, O. Leupold, Y. Shvyd'ko, G. V. Smirnov, R. Ruffer, Y. Inubushi, M. Yabashi, K. Tono, T. Kudo, and T. Ishikawa, *Superradiance of an ensemble of nuclei excited by a free electron laser*, Nat. Phys. **14**, 261 (2018).
- [39] Y. Shvyd'ko, R. Röhlsberger, O. Kocharovskaya, J. Evers, G. A. Geloni, P. Liu, D. Shu, A. Miceli, B. Stone, W. Hippler, B. Marx-Glowna, I. Uschmann, R. Loetzsch, O. Leupold, H.-C. Wille, I. Sergeev, M. Gerharz, X. Zhang, C. Grech, M. Guetg, V. Kocharyan, N. Kujala, S. Liu, W. Qin, A. Zozulya, J. Hallmann, U. Boesenberg, W. Jo, J. Möller, A. Rodriguez-Fernandez, M. Youssef, A. Madsen, and T. Kolodziej, *Resonant x-ray excitation of the nuclear clock isomer ^{45}Sc* , Nature **622**, 471 (2023).
- [40] S. Matinyan, *Lasers as a bridge between atomic and nuclear physics*, Physics Reports **298**, 199 (1998).
- [41] T. J. Bürvenich, J. Evers, and C. H. Keitel, *Nuclear quantum optics with x-ray laser pulses*, Phys. Rev. Lett. **96**, 142501 (2006).
- [42] A. Pálffy, J. Evers, and C. H. Keitel, *Electric-dipole-forbidden nuclear transitions driven by super-intense laser fields*, Phys. Rev. C **77**, 044602 (2008).
- [43] K. P. Heeg, *X-ray quantum optics with Mössbauer nuclei in thin-film cavities*, (2014).
- [44] A. Junker, A. Pálffy, and C. H. Keitel, *Cooperative effects in nuclear excitation with coherent x-ray light*, New Journal of Physics **14**, 085025 (2012).
- [45] T. Salditt and M. Osterhoff, *X-ray focusing and optics*, in *Nanoscale Photonic Imaging*, edited by T. Salditt, A. Egner, and D. R. Luke (Springer International Publishing, Cham, 2020) pp. 71–124.
- [46] F. Schenk, *Optimization of resonances for multilayer x-ray resonators*, Göttingen Series in X-ray Physics, Vol. 003 (Universitätsverlag Göttingen, Göttingen, 2011).
- [47] L. M. Lohse, P. Andrejić, S. Velten, M. Vassholz, C. Neuhaus, A. Negi, A. Panchwane, I. Sergeev, A. Pálffy, T. Salditt, and R. Röhlsberger, *Collective nuclear excitation dynamics in mono-modal x-ray waveguides*, (2024), arXiv:2403.06508 [quant-ph].
- [48] L. M. Lohse and P. Andrejić, *Nano-optical theory of planar x-ray waveguides*, Optics Express **32**, 9518 (2024).
- [49] H.-Y. Chen, S. Hoffmann, and T. Salditt, *X-ray beam compression by tapered waveguides*, Applied Physics Letters **106**, 194105 (2015).
- [50] Y.-H. Chen, P.-H. Lin, G.-Y. Wang, A. Pálffy, and W.-T. Liao, *Transient nuclear inversion by x-ray free electron laser in a tapered x-ray waveguide*, Phys. Rev. Res. **4**, L032007 (2022).
- [51] R. Röhlsberger, J. Evers, and S. Shwartz, *Quantum and nonlinear optics with hard x-rays*, in *Synchrotron Light Sources and Free-Electron Lasers: Accelerator Physics, Instrumentation and Science Applications*, edited by E. Jaeschke, S. Khan, J. R. Schneider, and J. B. Hastings (Springer International Publishing, Cham, 2014) pp. 1–28.
- [52] R. Röhlsberger and J. Evers, *Quantum optical phenomena in nuclear resonant scattering*, in *Modern Mössbauer Spectroscopy*, edited by Y. Yoshida and G. Langouche (Springer Singapore, Singapore, 2021) pp. 105–171.

- [53] R. Röhlberger, K. Schlage, T. Klein, and O. Leupold, *Accelerating the spontaneous emission of x rays from atoms in a cavity*, Phys. Rev. Lett. **95**, 097601 (2005).
- [54] K. P. Heeg and J. Evers, *X-ray quantum optics with Mössbauer nuclei embedded in thin-film cavities*, Phys. Rev. A **88**, 043828 (2013).
- [55] D. Lentrodt, K. P. Heeg, C. H. Keitel, and J. Evers, *Ab initio quantum models for thin-film x-ray cavity QED*, Phys. Rev. Research **2**, 023396 (2020).
- [56] O. Diekmann, D. Lentrodt, and J. Evers, *Inverse design approach to x-ray quantum optics with mössbauer nuclei in thin-film cavities*, Phys. Rev. A **105**, 013715 (2022).
- [57] K. P. Heeg, C. H. Keitel, and J. Evers, *Inducing and detecting collective population inversions of mössbauer nuclei*, (2016), arXiv:1607.04116 [quant-ph].
- [58] See Companion paper at <https://arxiv.org/abs/2405.12780>.
- [59] A. Asenjo-Garcia, J. D. Hood, D. E. Chang, and H. J. Kimble, *Atom-light interactions in quasi-one-dimensional nanostructures: A Green's-function perspective*, Phys. Rev. A **95**, 033818 (2017).
- [60] C. D. Mink and M. Fleischhauer, *Collective radiative interactions in the discrete truncated Wigner approximation*, SciPost Phys. **15**, 233 (2023).
- [61] J. Schachenmayer, A. Pikovski, and A. M. Rey, *Many-body quantum spin dynamics with monte carlo trajectories on a discrete phase space*, Phys. Rev. X **5**, 011022 (2015).
- [62] M. Moreno-Cardoner, D. Goncalves, and D. E. Chang, *Quantum nonlinear optics based on two-dimensional rydberg atom arrays*, Phys. Rev. Lett. **127**, 263602 (2021).
- [63] J. Amann, W. Berg, V. Blank, F.-J. Decker, Y. Ding, P. Emma, Y. Feng, J. Frisch, D. Fritz, J. Hastings, Z. Huang, J. Krzywinski, R. Lindberg, H. Loos, A. Lutman, H.-D. Nuhn, D. Ratner, J. Rzepiela, D. Shu, Y. Shvyd'ko, S. Spampinati, S. Stoupin, S. Terentyev, E. Trakhtenberg, D. Walz, J. Welch, J. Wu, A. Zholents, and D. Zhu, *Demonstration of self-seeding in a hard-x-ray free-electron laser*, Nature Photonics **6**, 693 (2012).
- [64] I. Nam, C.-K. Min, B. Oh, G. Kim, D. Na, Y. J. Suh, H. Yang, M. H. Cho, C. Kim, M.-J. Kim, C. H. Shim, J. H. Ko, H. Heo, J. Park, J. Kim, S. Park, G. Park, S. Kim, S. H. Chun, H. Hyun, J. H. Lee, K. S. Kim, I. Eom, S. Rah, D. Shu, K.-J. Kim, S. Terentyev, V. Blank, Y. Shvyd'ko, S. J. Lee, and H.-S. Kang, *High-brightness self-seeded x-ray free-electron laser covering the 3.5 keV to 14.6 keV range*, Nature Photonics **15**, 435 (2021).
- [65] S. Liu, C. Grech, M. Guetg, S. Karabekyan, V. Kocharyan, N. Kujala, C. Lechner, T. Long, N. Mirian, W. Qin, S. Serkez, S. Tomin, J. Yan, S. Abeghyan, J. Anton, V. Blank, U. Boesenberg, F. Brinker, Y. Chen, W. Decking, X. Dong, S. Kearney, D. La Civita, A. Madsen, T. Maltezopoulos, A. Rodriguez-Fernandez, E. Saldin, L. Samoylova, M. Scholz, H. Sinn, V. Sleziona, D. Shu, T. Tanikawa, S. Terentiev, A. Trebushinin, T. Tschentscher, M. Vannoni, T. Wohlenberg, M. Yakopov, and G. Geloni, *Cascaded hard x-ray self-seeded free-electron laser at megahertz repetition rate*, Nature Photonics **17**, 984 (2023).
- [66] S. L. McCall and E. L. Hahn, *Self-induced transparency by pulsed coherent light*, Phys. Rev. Lett. **18**, 908 (1967).
- [67] J. Eberly, *Area theorem rederived*, Opt. Express **2**, 173 (1998).
- [68] B. W. Shore, *Manipulating Quantum Structures Using Laser Pulses* (Cambridge University Press, 2011).
- [69] L. Allen and J. Eberly, *Optical Resonance and Two-level Atoms*, Dover books on physics and chemistry (Dover, 1987).
- [70] See Supplemental Material at XXXX for details on the numerical algorithm to compute the field enhancement of focused x-ray beams in thin-film cavities.
- [71] R. Röhlberger, H. Thomas, K. Schlage, E. Burkel, O. Leupold, and R. Ruffer, *Imaging the magnetic spin structure of exchange-coupled thin films*, Phys. Rev. Lett. **89**, 237201 (2002).
- [72] T. Tschentscher, C. Bressler, J. Grünert, A. Madsen, A. P. Mancuso, M. Meyer, A. Scherz, H. Sinn, and U. Zastra, *Photon beam transport and scientific instruments at the european xfel*, Applied Sciences **7** (2017), 10.3390/app7060592.
- [73] A. Madsen, J. Hallmann, G. Ansaldi, T. Roth, W. Lu, C. Kim, U. Boesenberg, A. Zozulya, J. Möller, R. Shayduk, M. Scholz, A. Bartmann, A. Schmidt, I. Lobato, K. Sukharnikov, M. Reiser, K. Kazarian, and I. Petrov, *Materials Imaging and Dynamics (MID) instrument at the European X-ray Free-Electron Laser Facility*, Journal of Synchrotron Radiation **28**, 637 (2021).
- [74] A. Madsen, J. Hallmann, T. Roth, and G. Ansaldi, Technical design report - scientific instrument mid, https://www.xfel.eu/sites/sites_custom/site_xfel/content/e35165/e46561/e46883/e46942/e46945/xfel_file46946/TR-2013-005_TDR_MID_eng.pdf (2013), accessed: 2021-07-25.
- [75] M. Nakatsutsumi, K. Appel, G. Priebe, I. Thorpe, A. Pelka, B. Muller, and T. Tschentscher, Technical design report - scientific instrument hed, https://www.xfel.eu/sites/sites_custom/site_xfel/content/e35165/e46561/e46886/e46954/e46959/xfel_file46960/TR-2014-001_TDR_HED_eng.pdf (2014), accessed: 2021-07-25.
- [76] B. Adams, G. Aeppli, T. Allison, A. Q. R. Baron, P. Bucksbaum, A. I. Chumakov, C. Corder, S. P. Cramer, S. DeBeer, Y. Ding, J. Evers, J. Frisch, M. Fuchs, G. Grübel, J. B. Hastings, C. M. Heyl, L. Holberg, Z. Huang, T. Ishikawa, A. Kaldun, K.-J. Kim, T. Kolodziej, J. Krzywinski, Z. Li, W.-T. Liao, R. Lindberg, A. Madsen, T. Maxwell, G. Monaco, K. Nelson, A. Pallfy, G. Porat, W. Qin, T. Raubenheimer, D. A. Reis, R. Röhlberger, R. Santra, R. Schoenlein, V. Schünemann, O. Shpyrko, Y. Shvyd'ko, S. Shwartz, A. Singer, S. K. Sinha, M. Sutton, K. Tamasaku, H.-C. Wille, M. Yabashi, J. Ye, and D. Zhu, Scientific opportunities with an x-ray free-electron laser oscillator, (2019), arXiv:1903.09317 [physics.ins-det].
- [77] Scientific instrument mid, [Online; accessed 02-April-2024].
- [78] R. Follath, T. Koyama, V. Lipp, N. Medvedev, K. Tono, H. Ohashi, L. Patthey, M. Yabashi, and B. Ziaja, *X-ray induced damage of b4c-coated bilayer materials under various irradiation conditions*, Scientific Reports **9**, 2029 (2019).
- [79] J. Kim, A. Nagahira, T. Koyama, S. Matsuyama, Y. Sano, M. Yabashi, H. Ohashi, T. Ishikawa, and K. Yamauchi, *Damage threshold of platinum/carbon multilayers under hard x-ray free-electron laser irradiation*, Opt. Express **23**, 29032 (2015).

- [80] D. Lentrodt, Ab initio approaches to x-ray cavity qed, (2021).
- [81] C. R. Harris, K. J. Millman, S. J. van der Walt, R. Gommers, P. Virtanen, D. Cournapeau, E. Wieser, J. Taylor, S. Berg, N. J. Smith, R. Kern, M. Picus, S. Hoyer, M. H. van Kerkwijk, M. Brett, A. Haldane, J. Fernández del Río, M. Wiebe, P. Peterson, P. Gérard-Marchant, K. Sheppard, T. Reddy, W. Weckesser, H. Abbasi, C. Gohlke, and T. E. Oliphant, *Array programming with NumPy*, *Nature* **585**, 357–362 (2020).
- [82] P. Virtanen, R. Gommers, T. E. Oliphant, M. Haberland, T. Reddy, D. Cournapeau, E. Burovski, P. Peterson, W. Weckesser, J. Bright, S. J. van der Walt, M. Brett, J. Wilson, K. J. Millman, N. Mayorov, A. R. J. Nelson, E. Jones, R. Kern, E. Larson, C. J. Carey, Í. Polat, Y. Feng, E. W. Moore, J. VanderPlas, D. Laxalde, J. Perktold, R. Cimrman, I. Henriksen, E. A. Quintero, C. R. Harris, A. M. Archibald, A. H. Ribeiro, F. Pedregosa, P. van Mulbregt, and SciPy 1.0 Contributors, *SciPy 1.0: Fundamental Algorithms for Scientific Computing in Python*, *Nature Methods* **17**, 261 (2020).
- [83] J. D. Hunter, *Matplotlib: A 2d graphics environment*, *Computing in Science & Engineering* **9**, 90 (2007).